A Numerical Predictability Problem in Solution of the Nonlinear Diffusion Equation

PHILIP S. BROWN, JR., AND JOSEPH P. PANDOLFO

The Center for the Environment and Man, Inc., Hartford, CT 06120

(Manuscript received 13 February 1981; in final form 15 October 1981)

ABSTRACT

A numerical analysis of the nonlinear heat diffusion equation has been carried out to bring to light a heretofore little-understood type of instability that can be encountered in many numerical modeling applications. The nature of the instability is such that the error remains bounded but becomes large enough to prevent proper assessment of model results. For the sample problem under investigation, the nonlinearity is introduced through a diffusion coefficient that depends on the Richardson number which, in turn, is a function of the dependent variable. Our analysis shows that the interaction of short-wavelength and intermediate-wavelength solution components can induce nonlinear instability if the amplitude of either component is sufficiently large. Since the unstable solution may not wander far from the true solution, the error can be difficult to detect. A criterion, given in terms of a restriction on the Richardson number, guarantees local (short-term) stability of the numerical scheme whenever the criterion is satisfied. Numerical results obtained using a boundary-layer model with GATE Phase III data are presented to support the theoretical conclusions.

1. Introduction

The nonlinear transport/diffusion equation has been the focus of various investigations dealing with the occurrence of multiple equilibrium states in the long-range forecasting problem. An equilibrium state is *stable* if small departures from equilibrium remain small in time and *unstable* if small departures grow large in time. In this article we analyze for stability a particular finite-difference representation of the nonlinear diffusion equation. For the discrete problem under investigation, several steady states are identified and all but one shown to be unstable. The multiplicity of equilibria introduced by discretization then can compound the problem of dealing with the multiple equilibria that may be dictated by the physics.

A criterion, independent of the time step, is derived to guarantee that the solution will be stable in that the linearized equations governing the individual (Fourier) solution components permit only exponentially damping solutions. Instability problems (growing solution components) are avoided by maintaining sufficient distance from the unstable equilibria. The theoretical criterion is shown to be in close agreement with empirical results obtained with a detailed, one-dimensional, air–sea interaction model using data from the GATE Phase III period. When the stability criterion is violated, the nonlinear instability appears as an irregularly fluctuating, non-catastrophic error that becomes graphically evident after about a one-day time-interval of integration.

2. Nonlinear analysis

a. The governing equation

The equation upon which we base this investigation is the nonlinear heat-diffusion equation

$$\frac{\partial T}{\partial t} = \frac{\partial}{\partial z}\left(K(T)\frac{\partial T}{\partial z}\right) \tag{1}$$

for $0 \leq t \leq \tau$, $0 \leq z \leq Z$, where t denotes time, z is the (vertical) spatial coordinate, T is temperature and K the diffusion coefficient. K is assumed to be a linear function of $\partial T/\partial z$ of the form

$$K(T) = K_0\left(1 - \gamma\frac{\partial T}{\partial z}\right), \tag{2}$$

where K_0, γ are positive constants in the appropriate units. This form for $K(T)$ is regarded as a first approximation to a physically derived K that depends on the Richardson number which, in turn, is a function of $\partial T/\partial z$.

Let T_j^n denote the finite-difference approximation to $T(t, z)$ for $t = n\Delta t$, $n = 0, 1, \ldots, N$ and $z = j\Delta z$, $j = 0, 1, \ldots, J$, where Δt and Δz are time and space increments, respectively. For our stability analysis we consider the two-level, implicit finite-difference approximation

$$\frac{T_j^{n+1} - T_j^n}{\Delta t} = \frac{K_j^n}{\Delta z}\left(\frac{T_{j+1}^{n+1} - T_j^{n+1}}{\Delta z}\right) - \frac{K_{j-1}^n}{\Delta z}\left(\frac{T_j^{n+1} - T_{j-1}^{n+1}}{\Delta z}\right), \tag{3}$$

0027-0644/82/091214-10$06.50

with the explicit K_j^n defined as

$$K_j^n = K_0\left[1 - \gamma\left(\frac{T_{j+1}^n - T_j^n}{\Delta z}\right)\right]. \quad (4)$$

The nonlinear stability analysis of (3) that follows is based upon the approach originally presented by Phillips (1959) who demonstrated the manner in which modes of different wavelength can interact to cause instability in numerical solution of the nonlinear vorticity equation. Phillips's approach was later used by Richtmyer and Morton (1967) to demonstrate the same phenomenon for the nonlinear advection equation.

In the manner of Richtmyer and Morton we seek solutions to (3) of the form

$$T_j^n = C_0^n + C_1^n \cos\pi j + C_2^n \cos\frac{\pi}{2} j + S^n \sin\frac{\pi}{2} j, \quad (5)$$

made up of a constant term, two-grid-interval waves and four-grid-interval waves. The solution procedure begins by substitution of (5) in (3) and (4). Use of the appropriate trigonometric identities allows all terms in the resulting equation to be written as linear combinations of the components appearing in (5). We then can equate coefficients of the individual Fourier components to arrive at the following system of nonlinear difference equations:

$$C_0^{n+1} - C_0^n = 0, \quad (6a)$$

$$C_1^{n+1} - C_1^n = -4\lambda_1 C_1^{n+1} + 2\lambda_2(C_2^n S^{n+1} + C_2^{n+1} S^n), \quad (6b)$$

$$C_2^{n+1} - C_2^n = -2\lambda_1 C_2^{n+1} + 4\lambda_2(C_1^n S^{n+1} + C_1^{n+1} S^n), \quad (6c)$$

$$S^{n+1} - S^n = -2\lambda_1 S^{n+1} + 4\lambda_2(C_1^n C_2^{n+1} + C_1^{n+1} C_2^n), \quad (6d)$$

where

$$\lambda_1 = \frac{K_0 \Delta t}{(\Delta z)^2} \quad \text{and} \quad \lambda_2 = \frac{\gamma}{\Delta z}\lambda_1 . \quad (7a,b)$$

b. Stability of equilibrium points

Before examining the overall stability of the system (6), it is helpful to identify the equilibrium points for which $C_0^{n+1} = C_0^n = C_0$, $C_1^{n+1} = C_1^n = C_1$, etc., and then to examine the stability of the system in a neighborhood of each such point. In equilibrium, (6) becomes

$$C_0 = \text{constant}, \quad (8a)$$

$$0 = -4\lambda_1 C_1 + 4\lambda_2 C_2 S, \quad (8b)$$

$$0 = -2\lambda_1 C_2 + 8\lambda_2 C_1 S, \quad (8c)$$

$$0 = -2\lambda_1 S + 8\lambda_2 C_1 C_2 . \quad (8d)$$

Had we discretized only the spatial variable z and left time as a continuous variable, we would have arrived at a differential system, analogous to (6), having the form

$$\frac{dC_0}{dt} = 0, \quad (9a)$$

$$\frac{dC_1}{dt} = -4\hat{\lambda}_1 C_1 + 4\hat{\lambda}_2 C_2 S, \quad (9b)$$

$$\frac{dC_2}{dt} = -2\hat{\lambda}_1 C_2 + 8\hat{\lambda}_2 C_1 S, \quad (9c)$$

$$\frac{dS}{dt} = -2\hat{\lambda}_1 S + 8\hat{\lambda}_2 C_1 C_2 , \quad (9d)$$

where $\hat{\lambda}_i = \lambda_i/\Delta t$, $i = 1, 2$. The equilibrium equations for (9) have precisely the same form as (8) but with $\hat{\lambda}_i$ replacing λ_i, so that the temporally continuous system possesses the same equilibria found in the fully discrete system. Instability of equilibria in the temporally continuous case is found to carry over to the discrete analogue to portend stability problems regardless of the choice of time-differencing procedure.

The equilibrium points are easily found. Eq. (8b) implies that

$$C_1 = \frac{\lambda_2}{\lambda_1} C_2 S. \quad (10)$$

Substitution of (10) in (8c) and (8d) gives

$$0 = C_2\left(-2\lambda_1 + 8\frac{\lambda_2^2}{\lambda_1} S^2\right), \quad (11a)$$

$$0 = S\left(-2\lambda_1 + 8\frac{\lambda_2^2}{\lambda_1} C_2^2\right). \quad (11b)$$

These last three relations yield the five equilibrium solutions

$$(C_1, C_2, S) = \frac{\lambda_1}{\lambda_2} \times \begin{cases} (0, & 0, & 0) \\ (1/4, & 1/2, & 1/2) \\ (1/4, & -1/2, & -1/2) \\ (-1/4, & 1/2, & -1/2) \\ (-1/4, & -1/2, & 1/2) \end{cases} . \quad (12)$$

The character of the solution near these equilibrium points can serve to indicate the approximate location of the stability region, the boundary of which we wish to precisely delineate.

Because of the difficulty in dealing with a 3×3 system, we shall now restrict our attention to the subspace of solutions (C_1, C_2, S) that lie in the planes $C_2 = \pm S$. This will include the equilibrium points and all solutions for which $C_2^0 = \pm S^0$. The semicontinuous system (9) then becomes

$$\frac{dC_1}{dt} = -4\hat{\lambda}_1 C_1 \pm 4\hat{\lambda}_2 C_2^2, \tag{13a}$$

$$\frac{dC_2}{dt} = -2\hat{\lambda}_1 C_2 \pm 8\hat{\lambda}_2 C_1 C_2 . \tag{13b}$$

The corresponding discrete system is given in (A1a,b) in the Appendix. Since (13a,b) are of a simpler yet more general form than are the fully discrete equations, we consider in this section the stability of the equilibrium points for the semi-continuous case and relegate to the Appendix the more cumbersome analysis of the fully discrete case.

To carry out the analysis we first linearize (13) to determine the form of the Jacobian matrix associated with the system. If $\mathbf{C}_e$ is an equilibrium point $(C_1, C_2)_e$ of (13), its stability then can be determined from the sign of $\mathrm{Re}(\hat{\mu}_i)$, $i = 1, 2$ where $\hat{\mu}_1, \hat{\mu}_2$ are the eigenvalues of the Jacobian matrix evaluated at $\mathbf{C}_e$. If $\mathrm{Re}(\hat{\mu}_1) < 0$ for $i = 1, 2$, the equilibrium point is stable. In this case, any pair of solutions starting near $\mathbf{C}_e$ will remain close to each other and each will approach the equilibrium point as $t \to \infty$. If $\mathrm{Re}(\hat{\mu}_i) > 0$ for $i = 1$ or 2, the equilibrium point is unstable and solutions starting near $\mathbf{C}_e$ will diverge from $\mathbf{C}_e$.

Case i: $C_1 = C_2 = 0$

Here we find that

$$\hat{\mu}_1 = -4\hat{\lambda}_1, \hat{\mu}_2 = -2\hat{\lambda}_1 . \tag{14}$$

Since $\hat{\lambda}_1 > 0$, both eigenvalues are negative and the equilibrium point is stable. We can show in the same way that the origin $C_1 = C_2 = S = 0$ is a stable point for the general 3×3 system (i.e., without assuming $C_2 = \pm S$); this result is of considerable importance since stability for the two-dimensional case does not guarantee stability for the full system.

Case ii: $C_1 = \frac{1}{4}\hat{\lambda}_1/\hat{\lambda}_2$, $C_2 = \pm\frac{1}{2}\hat{\lambda}_1/\hat{\lambda}_2$

In this case the eigenvalues of the Jacobian matrix, with $C_2 = S$, take the form

$$\hat{\mu}_\pm = -2\hat{\lambda}_1(1 \pm \sqrt{5}). \tag{15}$$

Clearly $\mu_+ < 0$, $\mu_- > 0$ so that the equilibria are unstable (saddle points) and the system permits growing perturbations (diverging solutions).

Case iii: $C_1 = -\frac{1}{4}\hat{\lambda}_1/\hat{\lambda}_2$, $C_2 = \pm\frac{1}{2}\hat{\lambda}_1/\hat{\lambda}_2$

Here we consider the Jacobian matrix with $C_2 = -S$, and it follows in a manner similar to *Case ii* that the equilibrium points are saddle points, so that four out of the five equilibria are unstable.

It is shown in the Appendix that a completely analogous situation exists for the fully discrete system (6). Perturbation of (6) leads to a linearized system of the form

$$\mathbf{c}^{n+1} = \mathbf{A}^{-1}\mathbf{B}\mathbf{c}^n, \tag{16}$$

where

$$\mathbf{c}^n = \begin{pmatrix} {c_1}^n \\ {c_2}^n \end{pmatrix} \tag{17}$$

and where the amplification matrix $\mathbf{A}^{-1}\mathbf{B}$ is given in (A9). Since the solutions to the difference equation (16) are of the form μ^n, (16) is stable if and only if the eigenvalues μ_1, μ_2 of $\mathbf{A}^{-1}\mathbf{B}$ are ≤ 1 in modulus. It is shown that the origin of the (C_1, C_2) plane is a stable point while the surrounding equilibria are unstable in the same sense exhibited by the semi-continuous analogue. The close agreement with the semi-continuous case suggests a stability problem of a general nature that is not related to the particular time-differencing scheme chosen.[1]

Since it is the fully discrete case that we wish to test in the context of a numerical model, from this point on we concentrate our analysis on determining the stability region for the discrete system (6) and on developing a criterion that will force the solution to remain within this region.

c. *Delineation of the stability region*

We have now determined the stability characteristics of the five equilibrium points that have been identified: in the (C_1, C_2) plane (a composite of the two cases for which $C_2 = \pm S$), the origin represents a stable point positioned at the center of a rectangular region whose four vertices are saddle points. The configuration suggests that there may be some convex region centered at the origin within which the solution to (6) will be stable and outside of which the solution will be unstable. Because of the nature of the eigenvalues at the equilibrium points, we have sought a curve in the (C_1, C_2) plane on which $\mu_+ = +1$ and $-1 < \mu_- < 1$ as a boundary separating the stable and unstable regions. To find such a curve we refer to the equations derived in the Appendix and make the following simplifying assumption, viz. that the eigenvalues derived from the system (A3) may be approximated by those derived from (A4) for ${C_1}^{n+1} \approx {C_1}^n = C_1$ and ${C_2}^{n+1} \approx {C_2}^n = C_2$. For λ_1 sufficiently small this assumption is justified by the continuity of the eigenvalues as functions of the elements of the matrix (Ostrowski, 1960). Thus we proceed as for the equilibrium case, examining the eigenvalues of the matrix $\mathbf{A}^{-1}\mathbf{B}$ set forth in (A9).

The characteristic equation $|\mathbf{A}^{-1}\mathbf{B} - \mu| = 0$ for the case $C_2 = S$ takes the form

[1] Suggested by P. E. Long.

$$\left[\frac{(1 + 2\lambda_1 - 4\lambda_2 C_1 + 16\lambda_2^2 C_2^2}{\det\mathbf{A}} - \mu\right]$$

$$\times\left[\frac{(1 + 4\lambda_1 + 4\lambda_2 C_1 + 16\lambda_1\lambda_2 C_1 + 16\lambda_2^2 C_2^2)}{\det\mathbf{A}} - \mu\right]$$

$$\times\frac{-64\lambda_2^2 C_2^2(1 + \lambda_1)(1 + 2\lambda_1)}{(\det\mathbf{A})^2} = 0. \quad (18)$$

The discriminant D of this quadratic equation in μ then can be written as

$$D = (\det\mathbf{A})^{-2}4\{[\lambda_1 + 4\lambda_2 C_1(2\lambda_1 + 1)]^2 + 64\lambda_2^2 C_2^2(2\lambda_1 + 1)(\lambda_1 + 1)\} \quad (19)$$

so that $D > 0$ and both eigenvalues are real, supporting our conjecture as to the nature of μ_- and μ_+ on the boundary of the stability region and providing information as to the nature of the instability that is expected to occur whenever the point (C_1, C_2) lies outside the stability region. Any unstable solution component of (16) will be proportional to μ^n where $|\mu| > 1$. But if μ is real, μ^n can take on only one of two forms, viz. $|\mu|^n$ or $(-1)^n|\mu|^n$; thus the unstable component is locally an exponentially increasing function that is either unmodulated or modulated by a high-frequency, two-grid-interval wave.

It can be shown that for $\mu_+ = 1$, the characteristic equation (18) will be satisfied for all points on the curve defined by

$$C_1 = -\frac{2\lambda_2}{\lambda_1}C_2^2 + \frac{1}{4}\frac{\lambda_1}{\lambda_2}. \quad (20)$$

This result was derived by first locating several points on the curve, fitting a parabola to those points and then verifying the correctness of the result. When (20) is satisfied it can also be shown by straightforward examination of the solution that $-1 < \mu_- < +1$ so that (20) does, in fact, represent a locus of neutrally stable points. Other analytic considerations indicate that the system will be stable for all points in the (C_1, C_2) plane to the left of the parabola and unstable to the right of the curve on which $\mu_+ = +1$. Thus we would expect an unstable solution to exhibit locally an exponentially growing, low-frequency error. For the case $C_2 = -S$ a similar parabola is obtained but symmetric to (20) with respect to the λ_2 axis [i.e., λ_2 is replaced by $-\lambda_2$ in (20)] and with the stable region lying to the right of the curve. The combined stability region (the intersection of the stable regions for $C_2 = \pm S$) is indicated by the shaded area in Fig. 1. It is of interest to note that on the parabolas defined by

$$C_1 = -\frac{4\lambda_2}{1 + 4\lambda_1}C_2^2 \pm \frac{1 + 2\lambda_1}{4\lambda_2}, \quad (21)$$

the perturbation equations (16) are singular, corresponding to the situation in which $\det\mathbf{A} = 0$. The loci of singular lines for the case $\lambda_1 = 1$ are indicated by the long dashed curves in Fig. 1.

d. Numerical verification

To verify the results derived in the preceding sections, we have solved the system (6b–d) for various sets of initial conditions with $C_2^0 = S^0$ to produce a set of trajectories in the C_1, C_2 phase plane. The results for the case $\lambda_1 = \lambda_2 = 0.01$ are shown in Fig. 2. Near the saddle point it is seen that the trajectories are hyperbolic-type curves which approach the saddle point and then depart. Some trajectories then move toward the origin, the stable equilibrium. The dashed line indicates the boundary of the stability region and the dotted line indicates the boundary of the region in which $K > 0$. Accordingly, as long as the positivity requirement on K is satisfied, nonlinear instability can occur only in the shaded area shown in the figure. In Fig. 2, trajectories $\tau 1$ and $\tau 2$ are shown with connecting lines to illustrate how the distance between $\tau 1$ and $\tau 2$ increases with the iteration index n as the curves travel through the unstable region. Once both solutions have passed through the shaded area and enter the stable region, the distance between $\tau 1$ and $\tau 2$ approaches zero monotonically. The structure of the system prevents nonlinearly unstable solutions from becoming unbounded and constrains them to realistic values. Only by violating the basic assumption that $K > 0$ will solutions diverge from the origin.

e. A stability criterion

For practical considerations it now remains to translate our results involving C_1 and C_2 into a useful stability criterion for direct modeling application. We wish to restrict the amplitudes of the two- and four-grid-interval waves so that the point (C_1, C_2) lies within the shaded region of Fig. 1. To this end it is convenient to consider just two neighboring values of T_j and put bounds on (C_1, C_2) by limiting the size of $|T_j - T_{j-1}|$. Accordingly we consider $\Delta T_j \equiv T_j - T_{j-1}$ for the case $C_2 = S$ where T_j is of the form given in (5). We have

$$\Delta T_j = \begin{cases} -2C_1, & j \text{ odd} \\ 2(C_1 + C_2), & j = 4k, \quad k = 0, 1, 2, \cdots \\ 2(C_1 - C_2), & j = 4(k + \tfrac{1}{2}), \quad k = 0, 1, 2, \cdots \end{cases} \quad (22)$$

Suppose we require that $|\Delta T_j| \leq M$ for each j. Then, in particular,

$$\max_j |\Delta T_j| = 2|C_1| + 2|C_2| \leq M, \quad (23)$$

or

$$\frac{\lambda_2}{\lambda_1}|C_2| \leq -\frac{\lambda_2}{\lambda_1}|C_1| + \frac{1}{2}\frac{\lambda_2}{\lambda_1}M. \quad (24)$$

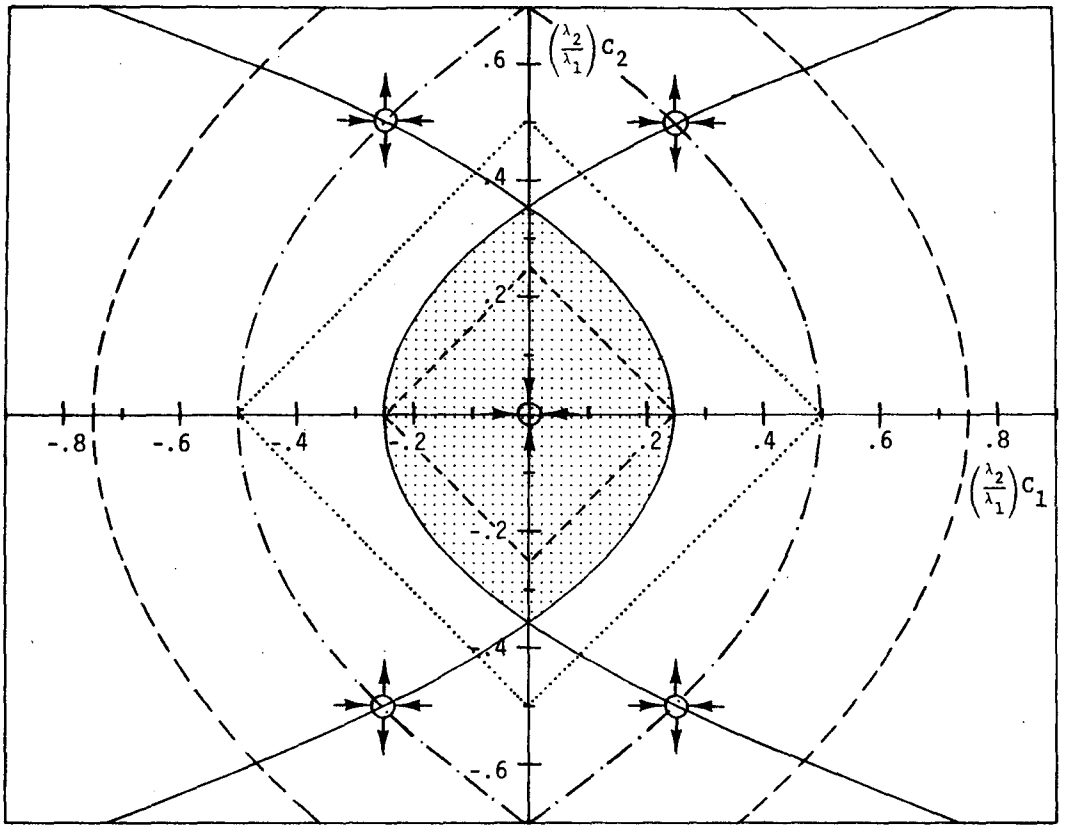

FIG. 1. The stability region (shaded area) for the nonlinear diffusion equation (3) as a subset of the (C_1, C_2) plane where C_1, C_2 are the amplitudes of two-grid-interval and four-grid-interval wave components, respectively. Equilibrium points are represented by the small circles with arrows indicating the stability characteristics of the points (incoming arrows indicating stability, outgoing arrows instability). Long-dashed and dot-dashed lines represent lines of singularities. Short-dashed lines delineate the stability region defined by inequality (24). Dotted lines delineate the region corresponding to the physical constraint $K > 0$.

The region defined by (24) is a diamond-shaped area centered at the origin of the (C_1, C_2) plane. We can make this area as large as possible and still remain within the stability region if we choose $M = \frac{1}{2}(\lambda_1/\lambda_2)$. The resulting subset of the stability region is outlined by the short dashed lines shown in Fig. 1. The criterion $|\Delta T_j| \leq \frac{1}{2}(\lambda_1/\lambda_2)$ now can be replaced by a convenient restriction on the Richardson number used in the calculation of K.

In the boundary-layer model used for this investigation as in many other meteorological models (see, e.g., Pandolfo, 1971) the functional form for $K(T)$ depends upon the existing condition of the local static stability of the physical system. In the atmosphere, for $\mathrm{Ri} \geq 0$, we use the formula

$$K = K_0(1 - |\alpha|\,\mathrm{Ri})^2, \tag{25}$$

while for $-1/(7|\alpha|) \leq \mathrm{Ri} < 0$,

$$K = K_0(1 + |\alpha|\,\mathrm{Ri})^{-3}. \tag{26}$$

For $\mathrm{Ri} < -\frac{1}{7}|\alpha|$, the formula for K does not involve the Richardson number and cannot be written in similar form. In the above expressions, α $(= -3)$ is the Monin-Obukhov constant and

$$\mathrm{Ri} \approx \Gamma \frac{\Delta T_j}{\Delta z} \tag{27}$$

where Γ is independent of T. If we now consider (25), the linear approximation to K corresponding to (4) is

$$K \approx K_0(1 - 2|\alpha|\mathrm{Ri}), \tag{28}$$

so that $\gamma = 2|\alpha|\Gamma$. (Here, $|\alpha||\mathrm{Ri}| < 1$.) Then the stability criterion

$$|\Delta T_j| < \frac{1}{2}(\lambda_1/\lambda_2) = \frac{\Delta z}{2\gamma} \tag{29}$$

for this case becomes

$$\mathrm{Ri} < \frac{1}{4|\alpha|}. \tag{30}$$

For the region corresponding to (26), we obtain in similar fashion the criterion $\mathrm{Ri} > -1/(6|\alpha|)$ which is automatically satisfied by the prescribed restriction

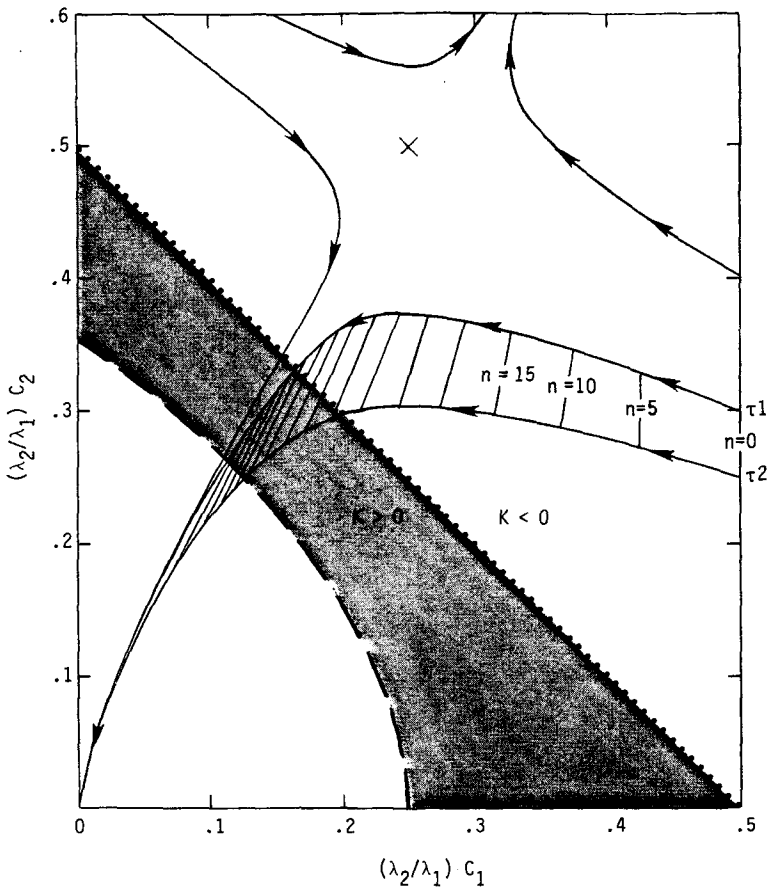

FIG. 2. Trajectories of solutions to (6b–d) in the non-dimensional C_1, C_2 phase plane. Dashed line denotes boundary of stability region, dotted line the boundary of the region in which $K > 0$. Cross marks position of saddle point while shaded area is subset of positive-K region in which nonlinear instability occurs. Distance between trajectories $\tau 1$ and $\tau 2$ increases with iteration index as curves pass through unstable region.

on the range of Ri. Thus (30) is the appropriate nonlinear stability criterion for the model formulation used in this study with the criterion applicable only for the case $\mathrm{Ri} \geqslant 0$. This restriction on Ri is more stringent than the physical bound, $\mathrm{Ri} < 1/(2|\alpha|)$ which guarantees that the diffusion coefficient be positive for the linearized K in (28). However, it is interesting to note that for the special form of K given in (2), the diffusion equation (1) can be written as[2]

$$\frac{\partial T}{\partial t} = K_0\left(1 - 2\gamma \frac{\partial T}{\partial z}\right)\frac{\partial^2 T}{\partial z^2}. \tag{31}$$

If $(1 - 2\gamma \partial T/\partial z)$ is now regarded as an effective diffusion coefficient $\tilde{K}$, the intuitively prescribed condition that this quantity be positive remarkably leads to (30), the derived nonlinear stability criterion. The result appears to be a coincidence since contrary to the intuitive notion regarding $\tilde{K}$, we can violate the condition $\tilde{K} > 0$ and still maintain damping solutions.[3] This result can be derived analytically by multiplying (1) by T and integrating over an interval (a, b) to arrive at the relation

$$\frac{1}{2}\frac{\partial}{\partial t}\int_a^b T^2 dz = TK\frac{\partial T}{\partial z}\bigg|_a^b - \int_a^b K\left(\frac{\partial T}{\partial z}\right)^2 dz. \tag{32}$$

If T or $\partial T/\partial z$ vanish at the end points, then the right-hand side of (32) will be <0 for all $K > 0$ and the solutions will damp in the mean. Damping will result, in particular, for

$$\frac{1}{2\gamma} < \frac{\partial T}{\partial z} < \frac{1}{\gamma}, \tag{33}$$

in which case $K > 0$ but $\tilde{K} < 0$.

The physical restriction $\mathrm{Ri} < 1/(2|\alpha|)$, correspond-

[2] Noted by one of the reviewers.

[3] This viewpoint was suggested by P. E. Long.

ing to the case $M = \lambda_1/\lambda_2$, implies that we always operate within the larger diamond-shaped region outlined by the dotted lines shown in Fig. 1 regardless of the stability considerations. Since the loci of singularities always lie outside this region, a singular amplification matrix cannot be encountered for finite values of λ_1 and positive values of K. In the limit as $\lambda_1 \to +\infty$, the loci of singularities contract, approaching the dot-dashed curves shown in Fig. 1.

f. Comments on the general case

The results thus far have been derived under the restrictive assumption that the solutions lie on the planes $C_2 = \pm S$ so that our stability diagram in Fig. 1 represents only a composite of the projections of these two planes on the (C_1, C_2) plane. Further work is needed to provide a complete picture of the stability region in (C_1, C_2, S) phase space. It is our conjecture that the stability region is a convex region centered at the origin, perhaps composed of intersecting paraboloids with axes lying along the C_1-axis. Stability then would require a bound on C_1 in conjunction with some combination of the amplitudes C_2, S of the four-grid-interval waves. Such a bound then could be translated into a restriction on the Richardson number in the manner described in Section 2e.

The conjecture is supported by some empirical results obtained by solving the system (6b–d) for initial conditions with $C_2^0 \neq \pm S^0$. Tests were performed similar to those described in Section 2d. In each experimental run, a pair of solutions was generated using closely spaced points for initial values to determine stability or instability according to whether the solutions converge or diverge. In qualitative terms, it was found that larger values of C_2 require smaller values of S in order to maintain stability.

3. Model experiments

A one-dimensional (vertical), air–sea interaction model has been used to test the theoretical results derived in the preceding sections in a practical setting. The model is an updated version of the one described by Pandolfo (1969) and used in a number of boundary-layer experiments (e.g., Pandolfo and Jacobs, 1972). The finite-difference equations governing the evolution of temperature and other dependent variables take the form of (3) but with adjustment for the nonuniformity of the grid and with incorporation of advection terms, forcing terms and appropriate exchange coefficients.

In the calculation of the horizontal pressure gradient, the model is known to contain a potential source of roundoff error due to the problem of summing terms of widely differing magnitude. As a test for our theory, we have run the model on the CRAY-1, with and without a double-precision option just for calculating the pressure gradients, in order to compare results from the more precise version of the model with those from the model in which a known source of roundoff error has been introduced. The object of the test is to verify that the error will grow only if our stability criterion (30) is violated. The roundoff error is analogous to the random perturbations used by Sutera (1980, 1981) in his study of the effects of stochastic noise on the solutions to dynamical systems having multiple equilibria.

In the experimental runs, the model has been used to simulate the two-day period, 0000 GMT ($=t_0$) September 4 1974 to 0000 GMT September 6 1974, using initial and boundary values derived from data gathered during the GATE Phase III period. Figs. 3a,b,c show three sets of forecast temperatures at the 25 m level as a function of time; solution values are plotted at 4-hour intervals (40 time steps) and the points joined by straight lines. In Fig. 3a the stability criterion is satisfied exactly and both solutions graphically coincide; Figs. 3b and 3c show the manner in which the single- and double-precision forecasts diverge as the criterion is violated to greater degrees. Analogous graphs for other height levels show qualitatively similar results. In all runs carried out with $\mathrm{Ri} < 1/(4|\alpha|)$ (not shown), all predicted quantities in single/double-precision comparison runs agreed to at least five significant figures throughout the forecast period. The dip in the temperature seen in Fig. 3b resulted from the occurrence of cloud formation that did not happen to take place in the runs depicted in Figs. 3a and 3c. Fig. 4 shows a detailed step-by-step plot of the solution values for the final 20 time steps for the runs depicted in Fig. 3c. It is seen that the single-precision run exhibits irregular fluctuations but does not depart far from the more accurate solution. The instability can persist for a long period of time due to many processes (e.g., advection, radiation) acting in the model to force the solution into the unstable region.

An alternative approach toward limiting the amplitudes of the two- and four-grid-interval waves as they affect the diffusion coefficient is simply to apply a smoothing operator to the vertical profile of K.[4] To test this approach, a three-point symmetric filter was applied to the K profile at each time step in a 48-hour run analogous to that of Fig. 3c (i.e., with the derived stability criterion not enforced). At the 25 m level, differences in the double- and single-precision solutions were at most 0.03°C, so that the filtering diminished the maximum error due to nonlinear instability by about an order of magnitude. At higher levels maximum differences, though also diminished, were still as large as 0.3°C. Thus filtering substantially reduces but does not eliminate the error growth due to the nonlinear instability.

[4] Suggested by P. E. Long.

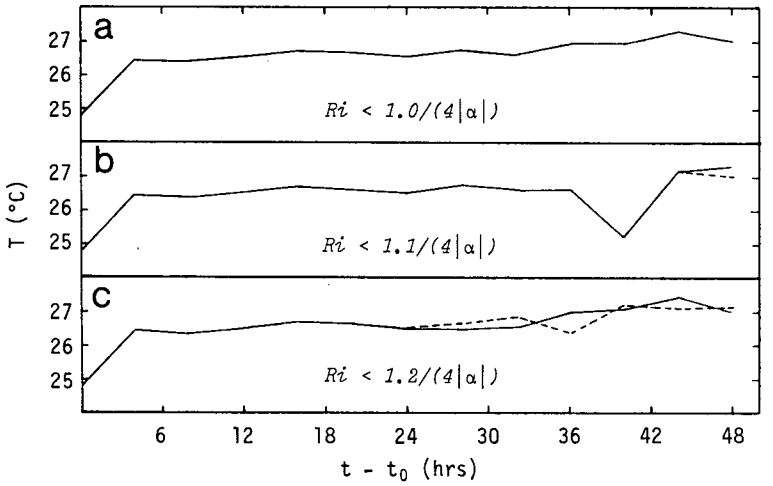

FIG. 3. Forecast temperatures at the 25 m level as a function of time. Solid lines indicate solutions obtained using high precision arithmetic; dashed lines indicate solution obtained with known source of roundoff error introduced. In (a) the stability criterion is satisfied exactly; in (b) and (c) the criterion is allowed to be violated by 10 and 20%, respectively.

4. Summary and conclusions

Predictability problems in long-term forecasting can be symptomatic of the presence of multiple stable and unstable equilibria which arise in the solution of the nonlinear advection/diffusion equations of meteorology. It is shown here that numerical solution of the nonlinear heat-diffusion equation can give rise to multiple equilibria as a result of aliasing and thereby compound the problems of predictability. A nonlinear numerical analysis has been performed using a trial solution of long-, intermediate- and short-wavelength components. Due to the limitations imposed by the discrete nature of the finite-difference approximation, interaction of these components can result in growing errors through the improper transfer of energy between different parts of the spectrum. The instability is characterized not by the familiar explosive growth of short-wavelength error but rather a meandering of the unstable solution about the true solution. Though not large, the error can cause considerable confusion in modeling efforts that involve sequences of complex programming changes. Stability does not depend on restricting the size of the time increment and is independent of the exact nature of the finite-difference scheme; stability depends instead on restricting the size of the amplitudes of the intermediate- and short-wavelength solution components. This latter type of criterion may be translated into a bound on the Richardson number which appears in the functional form of the diffusion coefficient. Alternatively, the error can be substantially reduced by applying a filter to the diffusion coefficients.

Further analyses of the nonlinear forecasting problem should include study of an overlay of the stability regions for both continuous and discrete problems to determine the extent to which the regions coincide; i.e., work should be aimed at establishing the degree of correspondence between the continuous predictability problem and its discrete analogue.

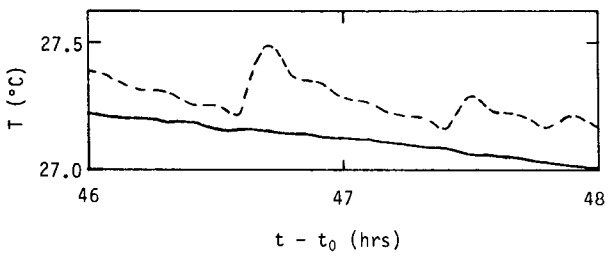

FIG. 4. As for Fig. 3c but with step-by-step plot for final 20 time steps.

Acknowledgments. This material is based upon work supported by the Division of Atmospheric Sciences, National Science Foundation under Grant ATM78-24273. Computing support was provided by the National Center for Atmospheric Research which is sponsored by the National Science Foundation. The authors are grateful to Dr. Alfonso Sutera who contributed to the research effort by allowing us to call upon his wide experience in the subject area, and to Dr. Paul Long and the reviewers for their valuable comments that led to improvement of the original manuscript. The authors also wish to thank Miss Phyllis Anderson for typing the manuscript and Miss Margaret Atticks for drafting the figures.

APPENDIX

Stability of Equilibrium Points for the Discrete Case

We wish to examine the stability of the discrete system (6) in a neighborhood of the equilibrium points (12). For $C_2 = \pm S$, (6) becomes

$$C_1^{n+1} - C_1^n = -4\lambda_1 C_1^{n+1} \pm 4\lambda_2 C_2^n C_2^{n+1}, \quad \text{(A1a)}$$

$$C_2^{n+1} - C_2^n = -2\lambda_1 C_2^{n+1} \pm 4\lambda_2 (C_1^n C_2^{n+1} + C_1^{n+1} C_2^n). \quad \text{(A1b)}$$

Choosing first the (+) sign in (A1) (corresponding to $C_2 = S$), we assume C_1, C_2 satisfy (A1) and consider a perturbed solution

$$\tilde{C}_1 = C_1 + c_1, \quad \tilde{C}_2 = C_2 + c_2 . \quad \text{(A2)}$$

The resulting linearized perturbation equations are

$$c_1^{n+1} - c_1^n = -4\lambda_1 c_1^{n+1} + 4\lambda_2 (c_2^n C_2^{n+1} + C_2^n c_2^{n+1}), \quad \text{(A3a)}$$

$$c_2^{n+1} - c_2^n = -2\lambda_1 c_2^{n+1} + 4\lambda_2 (c_1^n C_2^{n+1} + C_1^n c_2^{n+1} + c_1^{n+1} C_2^n + C_1^{n+1} c_2^n). \quad \text{(A3b)}$$

At equilibrium we have $C_1^{n+1} = C_1^n \equiv C_1$ and $C_2^{n+1} = C_2^n \equiv C_2$ in which case (A3) becomes

$$c_1^{n+1} - c_1^n = -4\lambda_1 c_1^{n+1} + 4\lambda_2 C_2 (c_2^n + c_2^{n+1}), \quad \text{(A4a)}$$

$$c_2^{n+1} - c_2^n = -2\lambda_1 c_2^{n+1} + 4\lambda_2 [C_2 (c_1^n + c_1^{n+1}) + C_1 (c_2^n + c_2^{n+1})]. \quad \text{(A4b)}$$

or in matrix form,

$$\mathbf{A}\mathbf{c}^{n+1} = \mathbf{B}\mathbf{c}^n, \quad \text{(A5)}$$

where

$$\mathbf{A} = \begin{pmatrix} 1 + 4\lambda_1 & -4\lambda_2 C_2 \\ -4\lambda_2 C_2 & 1 + 2\lambda_1 - 4\lambda_2 C_1 \end{pmatrix}, \quad \text{(A6)}$$

$$\mathbf{B} = \begin{pmatrix} 1 & 4\lambda_2 C_2 \\ 4\lambda_2 C_2 & 1 + 4\lambda_2 C_1 \end{pmatrix}, \quad \text{(A7)}$$

$$\mathbf{c}^n = \begin{pmatrix} c_1^n \\ c_2^n \end{pmatrix}. \quad \text{(A8)}$$

The difference equation (A5) will be stable if and only if the eigenvalues μ_1, μ_2 of $\mathbf{A}^{-1}\mathbf{B}$ have modulus $\leqslant 1$.

To find μ_1, μ_2 we first compute the amplification matrix $\mathbf{A}^{-1}\mathbf{B}$ as

$$(\det\mathbf{A})\mathbf{A}^{-1}\mathbf{B} = \begin{pmatrix} 1 + 2\lambda_1 - 4\lambda_2 C_1 + 16\lambda_2^2 C_2^2 & 8\lambda_2 C_2 (1 + \lambda_1) \\ 8\lambda_2 C_2 (1 + 2\lambda_1) & 1 + 4\lambda_1 + 4\lambda_2 C_1 + 16\lambda_1\lambda_2 C_1 + 16\lambda_2^2 C_2^2 \end{pmatrix}, \quad \text{(A9)}$$

where

$$\det\mathbf{A} = (1 + 4\lambda_1)(1 + 2\lambda_1 - 4\lambda_2 C_1) - 16\lambda_2^2 C_2^2. \quad \text{(A10)}$$

Case i: $C_1 = C_2 = 0$

For this equilibrium point, the off-diagonal elements of $\mathbf{A}^{-1}\mathbf{B}$ are zero and it follows directly that

$$\mu_1 = \frac{1}{1 + 4\lambda_1}, \quad \mu_2 = \frac{1}{1 + 2\lambda_1}. \quad \text{(A11)}$$

Since $\lambda_1 > 0$, $|\mu_1|$, $|\mu_2| < 1$ and the equilibrium point is stable. We can show in the same way that the origin $C_1 = C_2 = S = 0$ is a stable point for the general 3 $\times$ 3 system.

Case ii: $C_1 = \frac{1}{4}\frac{\lambda_1}{\lambda_2}$, $C_2 = \pm\frac{1}{2}\frac{\lambda_1}{\lambda_2}$

For this case

$$(\det\mathbf{A})\mathbf{A}^{-1}\mathbf{B} = \begin{pmatrix} 1 + \lambda_1 + 4\lambda_1^2 & \pm 4\lambda_1 (1 + \lambda_1) \\ \pm 4\lambda_1 (1 + 2\lambda_1) & 1 + 5\lambda_1 + 8\lambda_1^2 \end{pmatrix}, \quad \text{(A12)}$$

where

$$\det\mathbf{A} = 1 + 5\lambda_1 . \quad \text{(A13)}$$

The solutions to the quadratic characteristic equation (the same for either choice of C_2) take the form

$$\mu_\pm = (1 + 5\lambda_1)^{-1}\{1 + 3\lambda_1 + 6\lambda_1^2 \pm 2\lambda_1 [5 + 14\lambda_1 + 9\lambda_1^2]^{1/2}\}. \quad \text{(A14)}$$

Since the bracketed quantity [ ] is positive, both eigenvalues are real. Since [ ] also is >1, the solution corresponding to the positive square root satisfies the inequalities

$$\mu_+ > (1 + 5\lambda_1)^{-1}(1 + 5\lambda_1 + 6\lambda_1^2) > 1 \quad \text{(A15)}$$

and the system permits growing perturbations about the equilibrium points under consideration. To put bounds on the other eigenvalue, we write μ_- as

$$\mu_- = (1 + 5\lambda_1)^{-1}\left\{1 + 3\lambda_1 + 6\lambda_1^2 - 6\lambda_1^2\left[\frac{5}{9\lambda_1^2} + \frac{14}{9\lambda_1} + 1\right]^{1/2}\right\}. \quad \text{(A16)}$$

Then using the fact that $[\ \ ]^{1/2} > 1$, we have

$$\mu_- < \frac{1 + 3\lambda_1}{1 + 5\lambda_1} < 1. \tag{A17}$$

Furthermore,

$$\mu_- = (1 + 5\lambda_1)^{-1}\{1 + 3\lambda_1 + 6\lambda_1^2 - [20\lambda_1^2 + 56\lambda_1^3 + 36\lambda_1^4]^{1/2}\}, \tag{A18}$$

so that

$$\mu_- > (1 + 5\lambda_1)^{-1}\{1 + 3\lambda_1 + 6\lambda_1^2 - [64\lambda_1^2 + 96\lambda_1^3 + 36\lambda_1^4]^{1/2}\}, \tag{A19}$$

and finally

$$\mu_- > \frac{1 - 5\lambda_1}{1 + 5\lambda_1} > -1. \tag{A20}$$

Hence the equilibrium points are saddle points.

Case iii: $C_1 = -\frac{1}{4}\frac{\lambda_1}{\lambda_2}, \quad C_2 = \pm\frac{1}{2}\frac{\lambda_1}{\lambda_2}.$

We consider the perturbation equations corresponding to $C_2 = -S$ and, by the same argument given for Case ii, find that these equilibria are also saddle points.

REFERENCES

Ostrowski, A. M., 1960: *Solution of Equations and Systems of Equations*. Academic Press, 202 pp.

Pandolfo, J. P., 1969: Motions with inertial and diurnal period in a numerical model of the navifacial boundary layer. *J. Mar. Res.*, **27**, 301–317.

——, 1971: Numerical experiments with alternative boundary layer formulations using BOMEX data, *Bound.-Layer Meteor.*, **1**, 277–289.

——, and C. A. Jacobs, 1972: Numerical simulations of the tropical air–sea planetary boundary layer. *Bound.-Layer Meteor.*, **3**, 15–46.

Phillips, N. A., 1959: An example of non-linear computational instability. *The Atmosphere and the Sea in Motion*, Bolin, Ed., Rockefeller Institute Press, 501–504.

Richtmyer, R. D., and K. W. Morton, 1967: *Difference Methods for Initial-Value Problems*. Interscience, 405 pp.

Sutera, A., 1980: Stochastic perturbation of a pure convective motion. *J. Atmos. Sci.*, **37**, 245–249.

——, 1981: On stochastic perturbation and long-term climate behavior. *Quart. J. Roy. Meteor. Soc.*, **107**, 137–151.